ANALYSIS AND EXPERIMENTAL CHARACTERIZATION OF DAMAGED SHAFTS BY ONLINE AND OFFLINE EXCITATION

JOSÉ M. MACHORRO-LÓPEZ, DOUGLAS E. ADAMS,
School of Mechanical Engineering, Ray W. Herrick Laboratories
Purdue University

JULIO C. GÓMEZ-MANCILLA
Laboratory of Vibrations & Rotordynamics ESIME
National Polytechnic Institute

Abstract

Early detection of transverse cracks developing in shafts is crucial to avoid severe damage or even catastrophic failure of rotating machinery. In this paper, a 3D finite element model of an experimental rotating test rig is developed using ANSYS® with first order Timoshenko beam elements. Two different methods of modeling a crack in a very thin section at the middle of the shaft are considered by changing the geometric properties (open crack) and considering the breathing phenomenon using contact elements. External excitation on the inboard bearing is incorporated in the healthy system as well as in the damaged systems and the six vibratory responses are measured on the outboard bearing.

The results show that all the mode shapes (except the fifth) are identical for the damaged systems no matter how the crack is modeled; nevertheless, some differences in the natural

José M. Machorro-López, address: 140 S. Martin Jischke Drive, West Lafayette, IN 47907-2031, USA, phone: (765) 496-8438, fax: (765) 494-0787, e-mail: jmachorr@purdue.edu
Douglas E. Adams, address: 140 S. Martin Jischke Drive, West Lafayette, IN 47907-2031, USA, phone: (765) 496-6033, fax: (765) 494-0787, e-mail: deadams@purdue.edu
Julio C. Gómez-Mancilla, address: Av. IPN, Col. Lindavista, C.P. 07738, Mexico City, MEXICO, phone: (52-55) 5729-6000 Ext. 54737, fax: Ext. 54588, e-mail: jcgomez@ipn.mx

frequencies are observed between the two cracked shafts and also between the healthy shaft and the cracked shafts. Moreover, the healthy shaft has several mode shapes that are different than the cracked shafts and all modes of the healthy shaft are stable whereas the first two modes of the cracked shafts are unstable. Additionally, in most of the cases using external excitation, there is a significant increase in the torsional vibratory response around the longitudinal axis when an open crack exists; however, the breathing phenomenon almost completely inhibits the important torsional response. In this case, other vibratory responses, such as the horizontal response, are most useful for detecting the crack.

Introduction

High performance rotating equipment such as pumps, compressors, turbines, and engines all rely on shafts to transmit or receive power. Because shafts are often connected directly to the primary power supply for many mechanical systems, shafts experience severe operating conditions. Some of these conditions such as variations in temperature, speed, and torque make shafts susceptible to fatigue and can cause cracks to form. If these cracks are not detected, then total failure of the shaft can occur resulting in a large release of kinetic energy. For large equipment such as a gas or steam turbine, a fractured shaft could result in injuries and catastrophic damage to the facilities. For these reasons, researchers are continually trying to develop new and more reliable methods for detecting incipient cracks. Mayes and Davies [1], and Gasch [2] have studied the dynamics of a cracked rotor using simplified models, and Nelson and Nataraj [3] investigated the problem using the finite element method. Likewise, Saavedra and Cuitino [4] have developed a finite element model of a cracked shaft using a crack model, which introduced additional flexibility in the shaft through mechanisms of linear fracture mechanics.

This work focuses on analyzing two aspects to identify the presence of either an open crack or a breathing crack: a) the free response of the rotating systems, where mode shapes and natural frequencies are obtained numerically; and b) the off-line and on-line frequency domain vibratory response obtained at the outboard bearing (B2) of both systems (healthy and damaged) using external excitation on the inboard bearing (B1). The objective is to determine if and under what circumstances vibratory behavior can be used to detect cracking.

Finite element model

The Machinery Fault Simulator® (MFS) manufactured by Spectra Quest® is the experimental platform used in this work. The MFS has two ball bearings supporting a rotating shaft with two mounted discs and is designed to represent the behavior of real rotating equipment used by industry. To validate experimental results obtained with the MFS [5], a 3D finite element model with the dimensions and characteristics of the MFS apparatus is also developed in ANSYS®. **Fig. 1** shows a photograph of the MFS and the corresponding finite element model developed with ANSYS®.

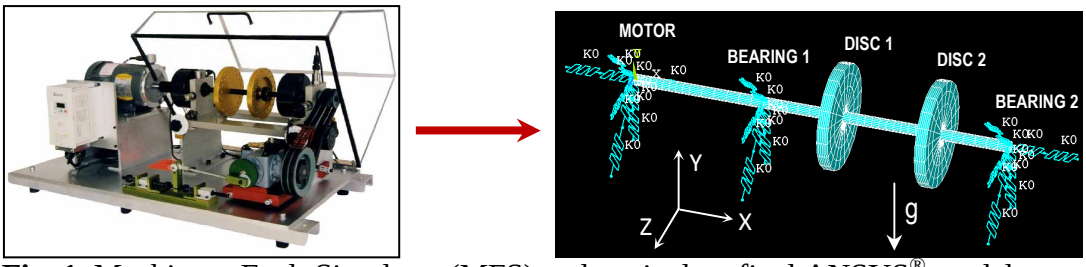

Fig. 1. Machinery Fault Simulator (MFS) and equivalent final ANSYS® model.

The numerical model was developed using beam189 elements to represent the shaft (which has a diameter of 0.016 m, a length between bearings of 0.365 m, and a length between the

motor and the inboard bearing of 0.195 m) and the two discs (each disc has a diameter of 0.152 m and a length of 0.016 m); the discs were modeled as solid elements with aluminum properties, whereas the properties of steel SAE 4140 were included for the shaft. Moreover, longitudinal springs in five different orientations using combin14 elements were implemented to represent the bearings and foundation, and a torsional spring, also using combin14, represents the flexible coupling between the motor and the inboard bearing. Additionally, the motor was modeled like a bearing having the same stiffness and damping properties of the bearings with which the shaft is supported; those stiffness and damping values were selected based on the geometry of the supports using strength of materials concepts. Furthermore, the gravitational field was modeled and Coriolis effects as well as so-called "spin softening" were taken into account for analyses with the shaft spinning.

To incorporate a transverse crack at shaft mid-span and analyze its effects when it remains always opened and when it is "breathing" (opening and closing), the following assumptions were made: 1) A geometric change was introduced in a thin transverse section at the middle of the shaft (crack thickness equal to 0.188e-3 m) to simulate an open crack; the cross-sectional area, moment of inertia, polar moment of inertia, and geometric center were modified using equations to represent an open crack with a depth of 25% of the shaft diameter [6]. 2) Contact elements type conta178 were implemented between the two nodes where the crack was assumed to exist (same location and thickness as in the open crack case) to simulate the crack breathing phenomenon. Most of the parameters for representing a breathing crack with a depth of 25% of the shaft diameter were calculated automatically by ANSYS taking into account several known properties of the material of the shaft. The parameters not calculated by ANSYS were estimated considering the experimental results obtained in [7].

Beam189 is a versatile quadratic element with 6 degrees of freedom (DOF) and 3 nodes and is based on Timoshenko's beam theory. Combin14 is a spring-damper element with longitudinal or torsional DOF in 3D; this element has no mass. Conta178 represents contact and sliding between any two nodes of any type of element; this element has 2 nodes with 3 DOF at each node and is capable of supporting compression in the contact normal direction and Coulomb friction in the tangential direction. Thus, the final model consists of 11 key points, 10 lines, 97 elements, and 153 nodes. Precise parameters to model an open crack are known and were implemented in the numerical model; however, the parameters to model a breathing crack were estimated as mentioned above. The two cases of cracks at the middle of the shaft (between bearings) studied in this paper and the cracks locations are illustrated in **Fig. 2**.

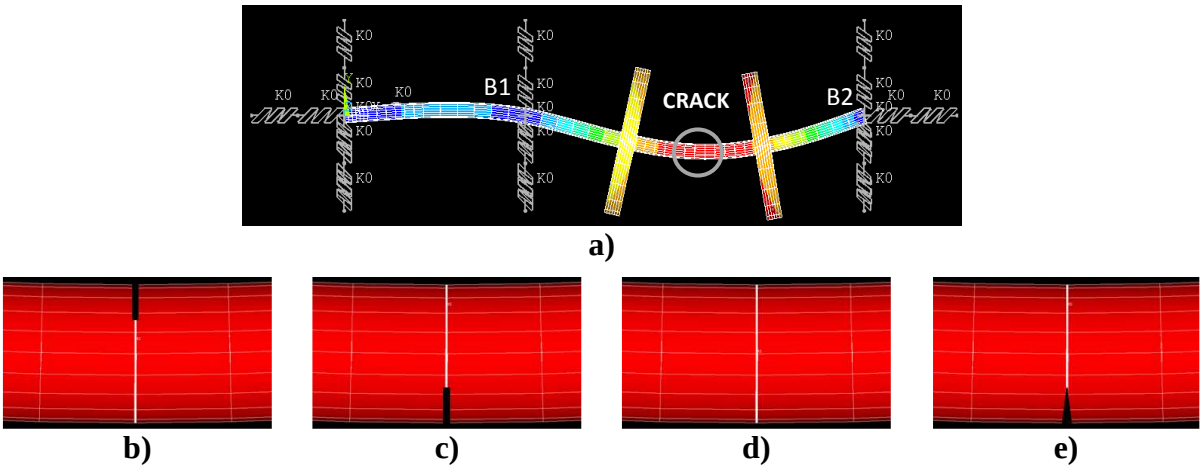

Fig. 2. Location of the damage in the rotating shaft and representation of the two kinds of cracks considered: **a)** crack at the shaft mid-span between bearings; **b)** open crack on the top part; **c)** open crack on the bottom part; **d)** breathing crack on the top part; **e)** breathing crack on the bottom part.

Results and discussion

A free response analysis was carried out on the rotating system with three shaft conditions. Campbell diagrams (to determine the natural frequencies and whether the modes are stable or unstable) and mode shapes were obtained. Changes in these characteristics could be used for structural assessment of rotating equipment to detect damaged shafts, but additional measurement and analysis procedures would be necessary.

In **Fig. 3**, Campbell diagrams from 0 to 10000 rpm are shown for the healthy system (**Fig. 3a**) and both damaged systems with open and breathing cracks (**Fig. 3b** and **3c** respectively). Some differences in the natural frequencies and stability can be observed by those plots and they are summarized in **Tab. 1**. The first two modes (torsional modes) of both cracked shafts are unstable at a very low frequency; in contrast, the healthy shaft does not exhibit instability.

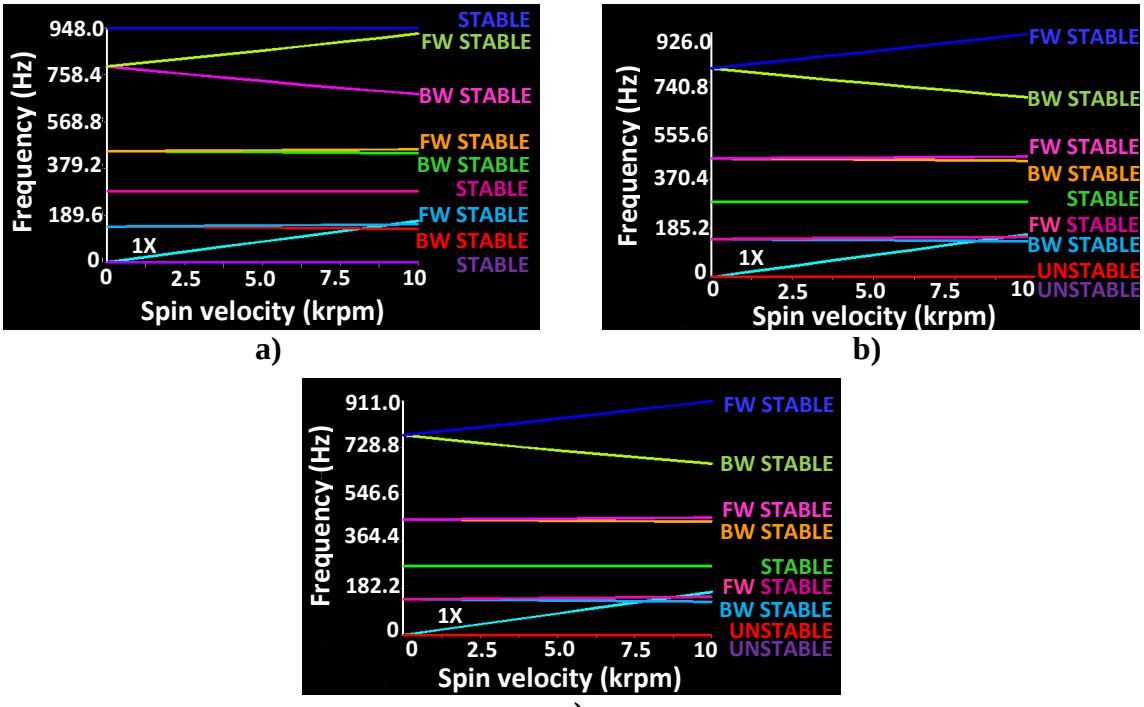

Fig. 3. Numerical Campbell diagrams: **a)** healthy shaft; **b)** open crack; **c)** breathing crack. FW=Forward, BW=Backward.

The corresponding mode shapes for each case (mode) from **Fig. 3** are shown in **Fig. 4**. Both cracked shafts revealed the same orbits and mode shapes for each comparable frequency, with the exception of the frequency corresponding to the fifth mode (torsional mode), where different behavior can be seen in the orbits (at a low speed) along the shaft. However, the healthy shaft shows several differences in the mode shapes with respect to the cracked shafts. The 1st, 3rd, 6th, and 8th modes have the same shape for healthy and damaged shafts, whereas the 2nd "healthy mode" corresponds to the 4th "damaged mode", and subsequently the 4th with the 5th (different orbital behavior is observed again in this torsional mode), the 5th with the 7th, and the 7th with the 9th.

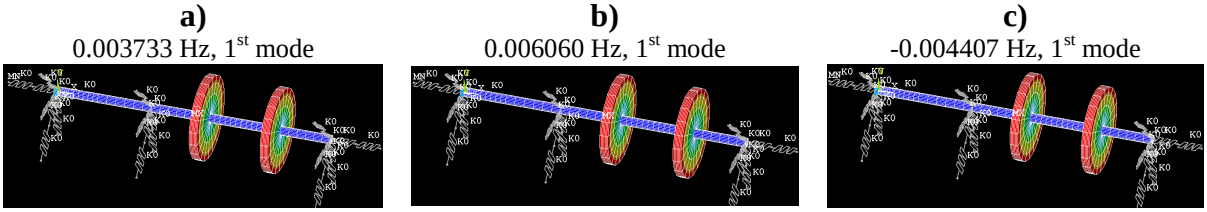

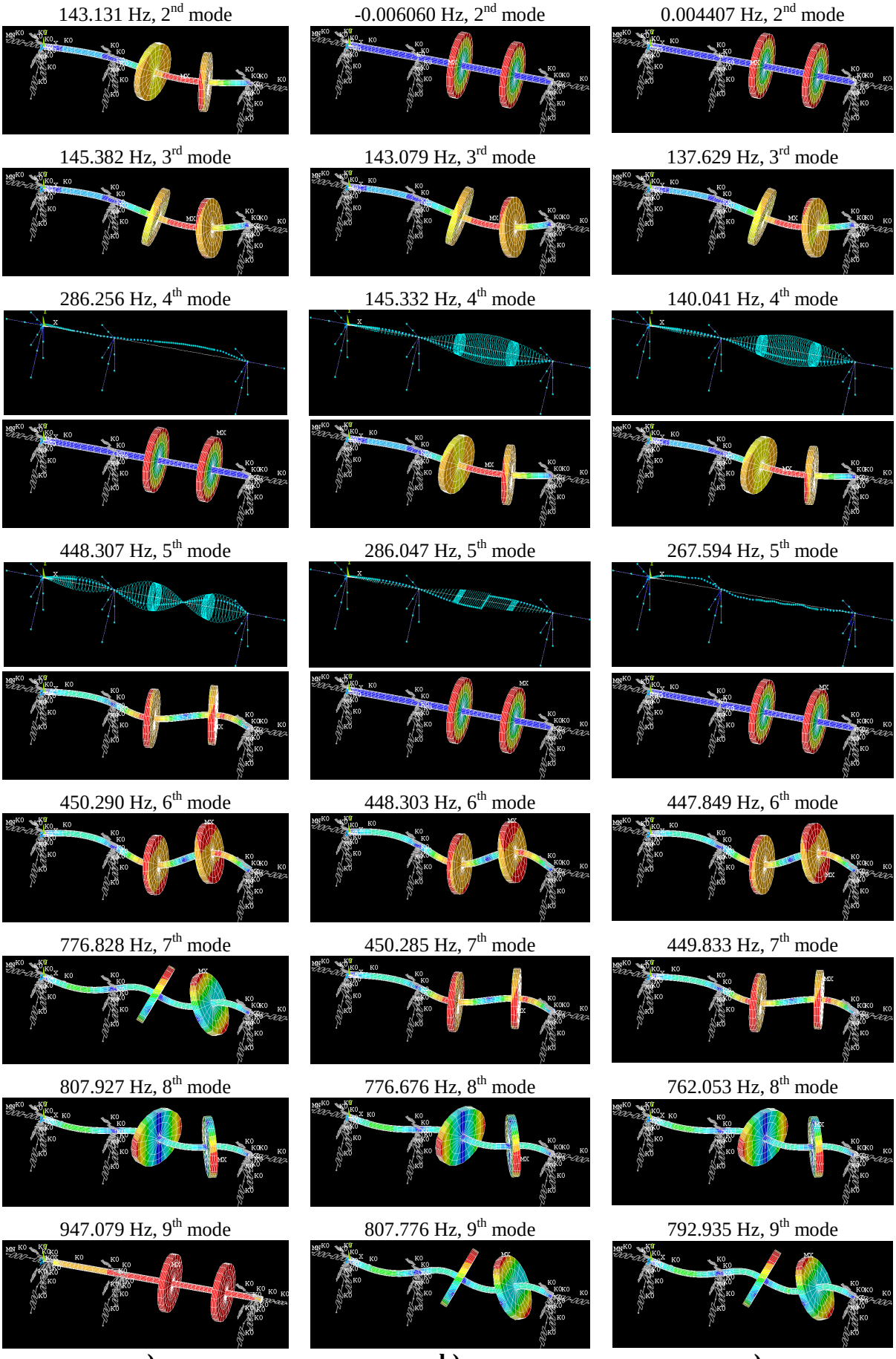

Fig. 4. Mode shapes: **a)** healthy shaft; **b)** open crack; **c)** breathing crack.

Tab. 1. Summary showing the natural frequencies and stability of the first nine modes for healthy shaft and both cracked shafts.

HEALTHY SHAFT	OPEN CRACK	BREATHING CRACK
0.003733 Hz (Stable)	***0.006060 Hz (Unstable)***	***-0.004407 Hz (Unstable)***
143.131 Hz (BW Stable)	***-0.006060 Hz (Unstable)***	***0.004407 Hz (Unstable)***
145.382 Hz (FW Stable)	143.079 Hz (BW Stable)	137.629 Hz (BW Stable)
286.256 Hz (Stable)	145.332 Hz (FW Stable)	140.041 Hz (FW Stable)
448.307 Hz (BW Stable)	***286.047 Hz (Stable)***	***267.594 Hz (Stable)***
450.290 Hz (FW Stable)	448.303 Hz (BW Stable)	447.849 Hz (BW Stable)
776.828 Hz (BW Stable)	450.285 Hz (FW Stable)	449.833 Hz (FW Stable)
807.927 Hz (FW Stable)	776.676 Hz (BW Stable)	762.053 Hz (BW Stable)
947.079 Hz (Stable)	807.776 Hz (FW Stable)	792.935 Hz (FW Stable)

FW=Forward, BW=Backward.

Because changes in the natural frequencies and mode shapes are a good indictator of serious structural damage, but neither conducive nor definitive in determining the presence of an incipient crack, in this work the use of an external excitation applied to one bearing when the system is off-line as well as on-line (shaft spining at 5000 rpm) is propossed. Excitation on the inboard bearing was implemented from 0 to 10 kHz in 6 directions (vertical, horizontal, axial, and torsional around X, Y, and Z axes) and the corresponding vibrational responses in the same 6 directions were obtained. Frequency vs. amplitude plots indicating with white circles the differences between healthy and damaged systems for each excitation case are shown in **Fig. 5** through **Fig. 16** and summarized in **Tab. 2**, where italic and bold letters are used to indicate the most convenient and promising scenarios to detect damage using experimental measurements.

When the system is off-line, vertical, axial, and torsional Z excitations are not useful to detect an open crack (see **Figs. 5a** and **5b**; **7a** and **7b**; and **10a** and **10b**); however, the torsional X response undergoes a significant change (increment of its amplitude) using horizontal or torsional Y excitations (see **Figs. 6a** and **6b**; and **9a** and **9b**); likewise, the horizontal and torsional Y responses are indicators to detect an open crack with a torsional X excitation that is applied off-line (see **Figs. 8a** and **8b**). For the on-line case, all the excitations, except the torsional X, produce a large increment in the torsional X response of the system with an open crack and this change in response can be used to detect the damage (see the cases **a)** and **b)** of **Figs. 11** to **16**). The breathing phenomenon of the crack makes it difficult to detect regardless of whether or not an external excitation is used; neverthless, the horizontal and torsional Y responses obtained with the incorporation of either horizontal or torsional Y excitations would be helpful to detect cracks with the system off-line (see **Figs. 6a** and **6c**; and **9a** and **9c**). The same responses would also be useful to detect the breathing crack with the system on-line, but with either torsional Y or torsional Z excitations (see **Figs. 15a** and **15c**; and **16a** and **16c**).

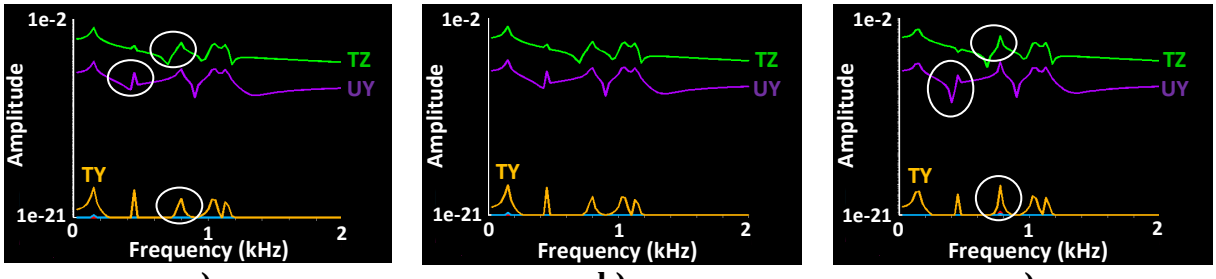

Fig. 5. Off-line vertical excitation on B1 and responses on B2: **a)** healthy shaft; **b)** open crack; **c)** breathing crack. UY=Vertical response, TY=Torsional Y response, TZ=Torsional Z response.

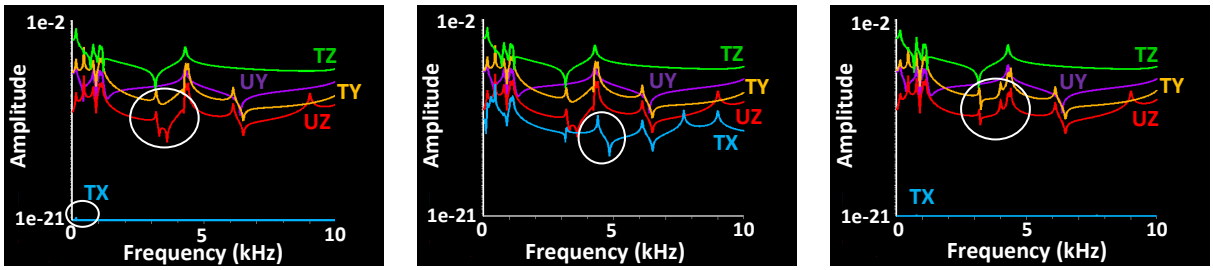

a) **b)** **c)**

Fig. 6. Off-line horizontal excitation on B1 and responses on B2: **a)** healthy shaft; **b)** open crack; **c)** breathing crack. UY=Vertical response, UZ=Horizontal response, TX=Torsional X response, TY=Torsional Y response, TZ=Torsional Z response.

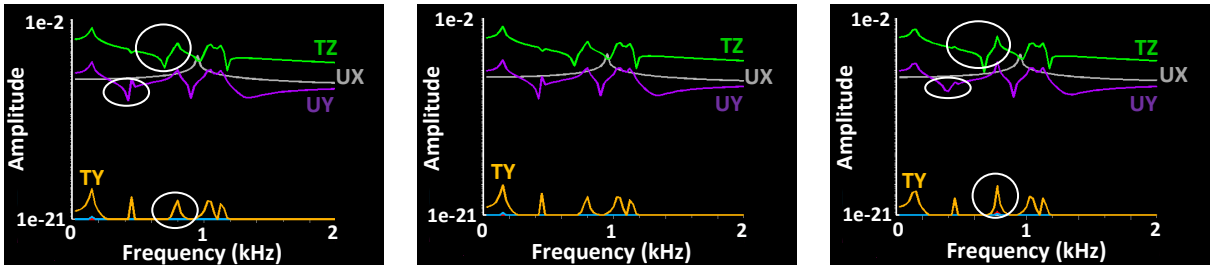

a) **b)** **c)**

Fig. 7. Off-line axial excitation on B1 and responses on B2: **a)** healthy shaft; **b)** open crack; **c)** breathing crack. UY=Vertical response, UX=Axial response, TY=Torsional Y response, TZ=Torsional Z response.

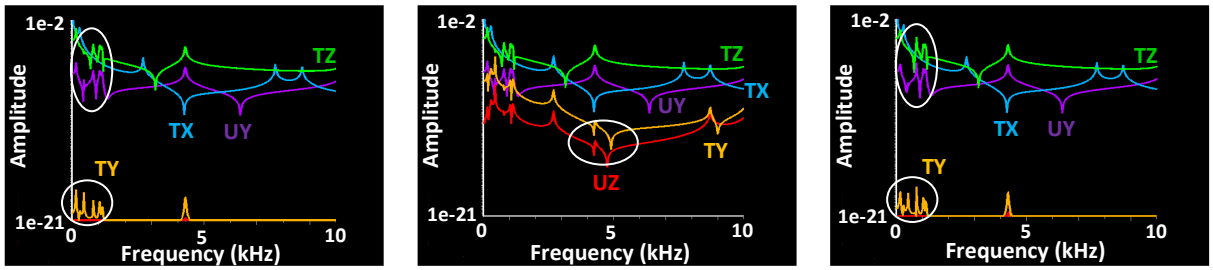

a) **b)** **c)**

Fig. 8. Off-line torsional X excitation on B1 and responses on B2: **a)** healthy shaft; **b)** open crack; **c)** breathing crack. UY=Vertical response, UZ=Horizontal response, TX=Torsional X response, TY=Torsional Y response, TZ=Torsional Z response.

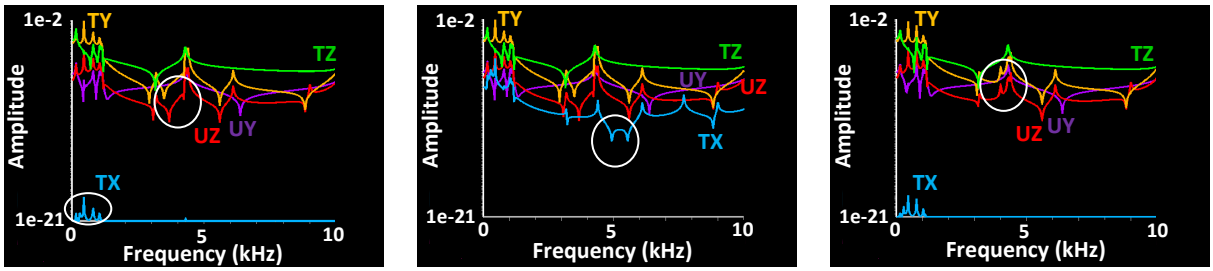

a) **b)** **c)**

Fig. 9. Off-line torsional Y excitation on B1 and responses on B2: **a)** healthy shaft; **b)** open crack; **c)** breathing crack. UY=Vertical response, UZ=Horizontal response, TX=Torsional X response, TY=Torsional Y response, TZ=Torsional Z response.

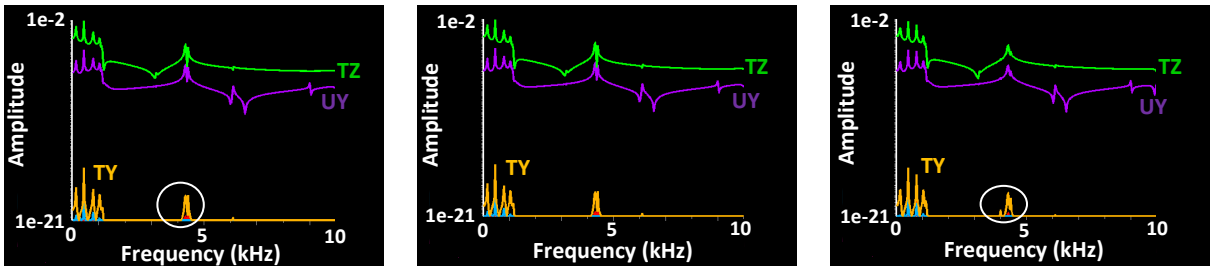

a) **b)** **c)**

Fig. 10. Off-line torsional Z excitation on B1 and responses on B2: **a)** healthy shaft; **b)** open crack; **c)** breathing crack. UY=Vertical response, TY=Torsional Y response, TZ=Torsional Z response.

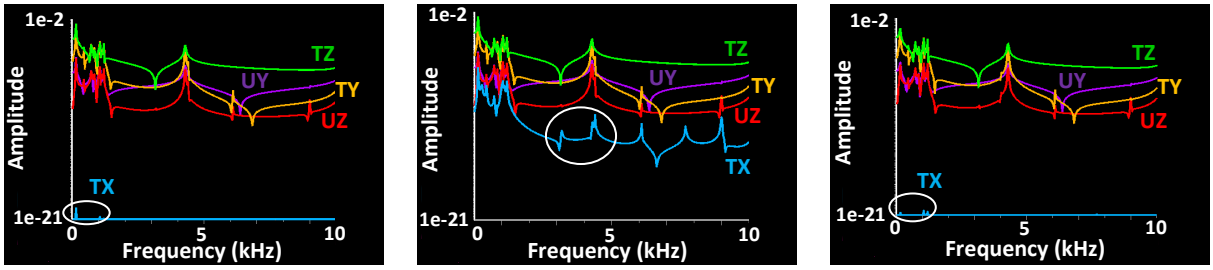

a) **b)** **c)**

Fig. 11. On-line vertical excitation on B1 and responses on B2: **a)** healthy shaft; **b)** open crack; **c)** breathing crack. UY=Vertical response, UZ=Horizontal response, TX=Torsional X response, TY=Torsional Y response, TZ=Torsional Z response.

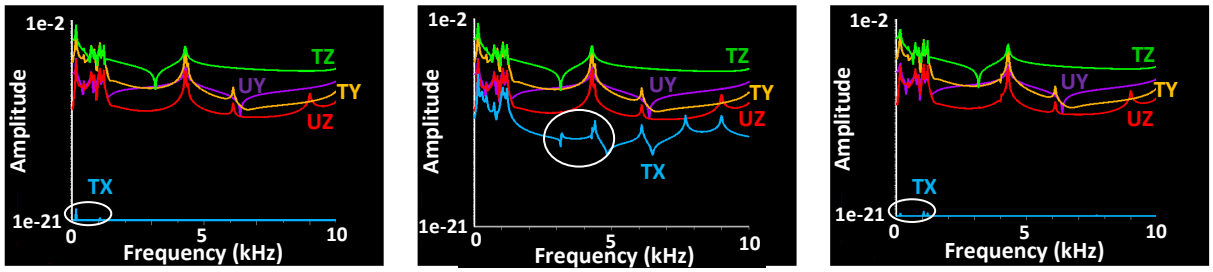

a) **b)** **c)**

Fig. 12. On-line horizontal excitation on B1 and responses on B2: **a)** healthy shaft; **b)** open crack; **c)** breathing crack. UY=Vertical response, UZ=Horizontal response, TX=Torsional X response, TY=Torsional Y response, TZ=Torsional Z response.

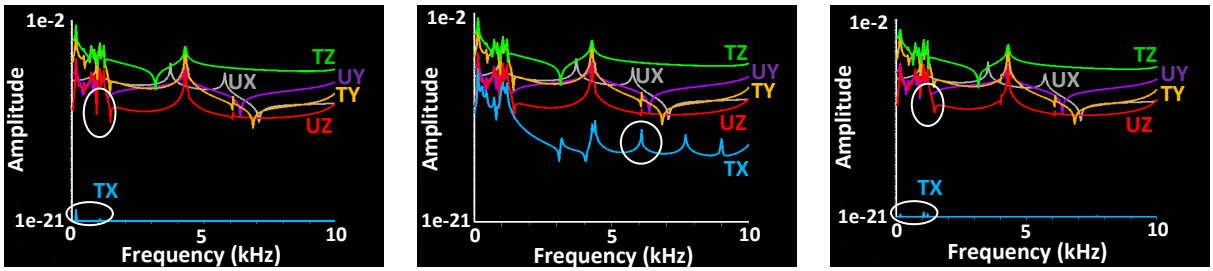

a) **b)** **c)**

Fig. 13. On-line axial excitation on B1 and responses on B2: **a)** healthy shaft; **b)** open crack; **c)** breathing crack. UY=Vertical response, UZ=Horizontal response, UX=Axial response, TX=Torsional X response, TY=Torsional Y response, TZ=Torsional Z response.

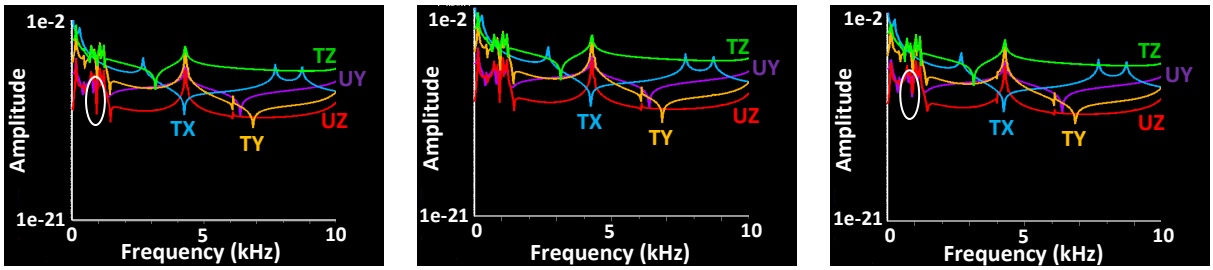

a) **b)** **c)**

Fig. 14. On-line torsional X excitation on B1 and responses on B2: **a)** healthy shaft; **b)** open crack; **c)** breathing crack. UY=Vertical response, UZ=Horizontal response, TX=Torsional X response, TY=Torsional Y response, TZ=Torsional Z response.

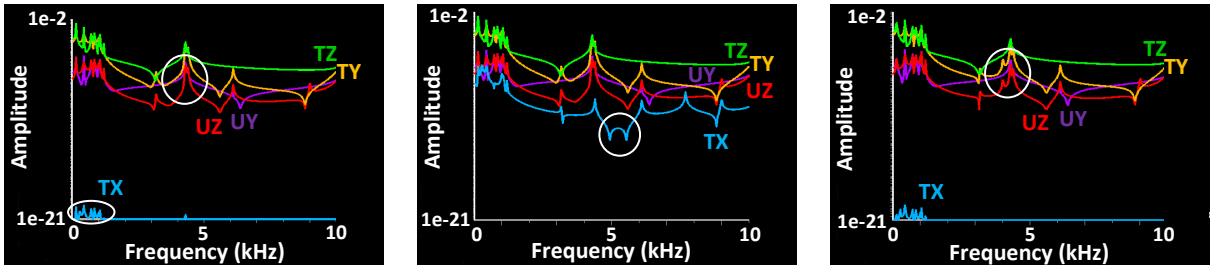

a) **b)** **c)**

Fig. 15. On-line torsional Y excitation on B1 and responses on B2: **a)** healthy shaft; **b)** open crack; **c)** breathing crack. UY=Vertical response, UZ=Horizontal response, TX=Torsional X response, TY=Torsional Y response, TZ=Torsional Z response.

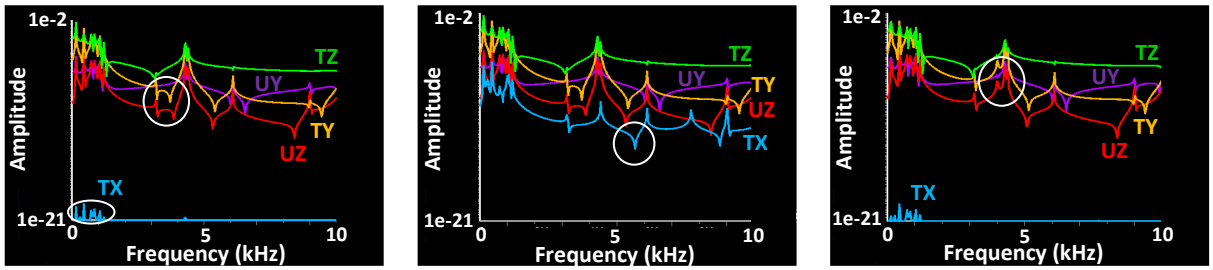

a) **b)** **c)**

Fig. 16. On-line torsional Z excitation on B1 and responses on B2: **a)** healthy shaft; **b)** open crack; **c)** breathing crack. UY=Vertical response, UZ=Horizontal response, TX=Torsional X response, TY=Torsional Y response, TZ=Torsional Z response.

Tab. 2. Summary showing the useful responses for detecting cracks using external excitation.

Off-line excitation	Open crack	Breathing crack	On-line excitation	Open crack	Breathing crack
-FY	-	UY, TY, TZ	-FY	***TX***	TX
-FZ	***TX***	***UZ, TY***	-FZ	***TX***	TX
-FX	-	UY, TY, TZ	-FX	***TX***	UZ, TX
-MX	***UZ, TY***	UY, TY, TZ	-MX	-	UZ
-MY	***TX***	***UZ, TY***	-MY	***TX***	***UZ, TY***
-MZ	-	TY	-MZ	***TX***	***UZ, TY***

FY=Vertical excitation, FZ=Horizontal excitation, FX=Axial excitation, MX=Torsional X excitation, MY=Torsional Y excitation, MZ=Torsional Z excitation; UY=Vertical response, UZ=Horizontal response, UX=Axial response, TX=Torsional X response, TY=Torsional Y response, TZ=Torsional Z response.

Conclusions

All natural frequencies of the rotating system were found to be similar for both open and breathing cracks, and the corresponding mode shapes were identical, except for the fifth

mode (torsional), where a small change was observed in the orbit plot at low speed. Likewise, the healthy system showed subtle changes in the natural frequencies and mode shapes with respect to the damaged systems. This analysis of the free response can be supplemented with on/off line excitation applied to a bearing to diagnose the presence of cracks in the shaft. Using external excitation, an open crack could be detected by analyzing the changes in the torsional X response. In contrast, a breathing crack was masked completely by observing the torsional X response. For this case, other responses were found to be most useful for detecting cracks such as the horizontal response. Nonlinear signal processing techniques, as opposed to the linear methods applied in this paper, are probably needed to detect breathing cracks.

Acknowledgments

The authors gratefully acknowledge the support offered by CONACYT.

References

[1] Mayes, I.W., Davies, W.G.R.: The vibrational behaviour of a rotating shaft system containing a transverse crack. Proceedings of the Institution of Mechanical Engineers, pp.53-64., London 1976.

[2] Gasch, R.: Dynamic behaviour of a simple rotor with a cross-sectional crack. Proceedings of the Institution of Mechanical Engineers, pp.123-128., London 1976.

[3] Nelson, H.D., Nataraj, C.: Dynamics of a rotor system with a cracked shaft. Journal of Vibration, Acoustics, Stress, and Reliability in Design, Vol.108, No.2, pp.189-196., 1986.

[4] Saavedra, P.N., Cuitino, L.A.: Vibration analysis of rotor for crack identification. Journal of Vibration and Control, Vol.8, No.1, pp.51-67., 2002.

[5] Adams, D.E., Gómez-Mancilla, J.C., Machorro-López, J.M.: Analysis and characterization of cracked shafts by online and offline external excitation. Purdue Systems Integrity for Defense Technology Summit, West Lafayette 2008.

[6] Jiménez-Rabiela, H., Urriolagoitia-Calderón, G., Hernández-Gómez, L.H.: Survey of the fracture in the rotor of the system rotor-mass-bearings. Proceedings of the 8° Congreso Nacional en Ingeniería Electromecánica y de Sistemas, pp.115-120., Mexico City 2004.

[7] García-Illescas, R., Gómez-Mancilla, J.C.: Dynamic behaviour of cracked shafts and signal processing of its vibratory response for steady crack growth detection. Proceedings of the 5th International Conference Acoustical and Vibratory Surveillance Methods and Diagnostic Techniques, pp.23-32., Senlis 2004.

ANALYSE UND EXPERIMENTELLE CHARAKTERISIERUNG VON GEBROCHENEN WELLEN MIT ONLINE- UND OFFLINE-ANREGUNGSMETHODEN

Zusammenfassung

In diesem Dokument wird ein 3D finites Element Modell von einem experimentellen rotierenden Prüfstand entwickelt. Das Modell wurde mit Timoshenko Stabelementen erster Ordnung in ANSYS® entwickelt. Zwei verschiedene Methoden der Modellierung des Bruches in einer sehr dünnen Abschnitt in der Mitte der Welle wurden beim Ändern der geometrischen Eigenschaften (geöffnete Brüche) und Berücksichtigen des Atmungs-Phänomen mit Kontaktelementen berücksichtigt. Externe Anregungen wurden in die Innenlager der schadensfreien und beschädigten Systeme eingeführt und sechs Schwingungsverhalten wurden im Außenlager gemessen. Die Ergebnisse zeigen dass in den meisten Fällen externer Anregung ein bedeutender Anstieg der Torsionsverhalten um die Längsachse zu verzeichnen ist wenn ein offener Bruch besteht. Das Atmungs-Phänomen verhindert jedoch fast vollständig die wichtige Torsionsverhalten. In diesem Fall sind andere Schwingungsverhalten sowie die Horizontalverhalten hilfreicher um Brüche zu detektieren.